Original Paper

Cells Tissues Organs

Cells Tissues Organs 2011;193:158–169
DOI: 10.1159/000318605

Accepted after revision: June 23, 2010
Published online: October 20, 2010

E-Cadherin and Transglutaminase-1 Epithelial Barrier Restoration Precedes Type IV Collagen Basement Membrane Reconstruction following Vocal Fold Mucosal Injury

Changying Ling Jennifer L. Raasch Nathan V. Welham

Department of Surgery, Division of Otolaryngology, University of Wisconsin School of Medicine and Public Health, Madison, Wisc., USA

Key Words
Tissue repair · Hyperplasia · Larynx · Reepithelialization · Wound healing · Rat

Abstract
The vocal fold epithelium is critical to upper airway immunologic defense and water/ion transport; therefore, any form of physical trauma or insult increases the vulnerability of this structure to functional impairment and pathogen invasion/infection. In this study, we examined the reestablishment of epithelial and basement membrane barrier structures in a well-established rat model of vocal fold mucosal injury. We observed active cell recruitment culminating in peak hyperplasia at 3 days postinjury, the establishment of robust E-cadherin+ and transglutaminase-1+ biochemical barrier signals along the epithelial surface by 3 days postinjury, and the persistent absence of a type IV collagen+ basement membrane at 7 days postinjury. The distinct spatial and temporal immunoactivity of these molecules is consistent with a programmed repair process driving the restoration of vocal fold mucosal integrity and permeability. These data may inform future efforts to optimize functional mucosal recovery postinjury and avoid undesirable events such as barrier compromise or epithelial metaplasia.

Introduction

The vocal fold mucosa, a layered structure comprised of epithelium and lamina propria (LP), is subject to a barrage of environmental challenges in the form of airflow turbulence [Khosla et al., 2008, 2009], biomechanical stress and strain [Gray et al., 1999, 2000], inhaled allergens and pathogens [Dworkin et al., 2009; Mouadeb et al., 2009], and gastric refluxate [Johnston et al., 2007; Birchall et al., 2008; Bulmer et al., 2010]. Its epithelial layer transitions from a stratified squamous cell formation to a cili-

Abbreviations used in this paper

ANOVA	analysis of variance
A-P	anterior-posterior
Col-IV	type IV collagen
CPF	ciliated pseudocolumnar formation
DAPI	4′,6-diamidino-2-phenylindole dihydrochloride
E-cad	E-cadherin
HE	hematoxylin and eosin
LP	lamina propria
M-L	medial-lateral
S-I	superior-inferior
SSC	stratified squamous cell
TGase-1	transglutaminase-1

KARGER

Fax +41 61 306 12 34
E-Mail karger@karger.ch
www.karger.com

Accessible online at:
www.karger.com/cto

Dr. Nathan V. Welham
Department of Surgery, Division of Otolaryngology
University of Wisconsin School of Medicine and Public Health
K4/723 CSC, 600 Highland Avenue, Madison, WI 53792 (USA)
Tel. +1 608 263 0121, Fax +1 608 252 0939, E-Mail welham@surgery.wisc.edu

ated pseudocolumnar cell formation along its superior-inferior (S-I) axis [Ling et al., 2010] and is primarily responsible for vocal fold immune, transport, and barrier functions [Sivasankar and Fisher, 2007; Leydon et al., 2009; Thibeault et al., 2009]. The physiologic and molecular mechanisms regulating these protective functions are poorly understood, particularly under conditions of epithelial compromise such as mucosal injury. Consequently, additional research is needed to better understand and optimize the restoration of vocal fold epithelial function in the context of overall mucosal repair.

We recently reported a significant alteration in rat vocal fold epithelial cell morphology and distribution following injury [Ling et al., 2010]. Reepithelialization was one of the earliest observable mucosal repair events and was completed by 3 days postinjury. The reconstructed epithelium was characterized by multiple layers of cells with enlarged cytoplasmic morphology, the return of superior and midpoint vocal fold squamous cell stratification by 7 days postinjury, and the complete absence of inferior vocal fold pseudocolumnar morphology through 7 days postinjury. These distinct and sequential morphological changes likely correspond to transient or permanent functional changes; however, the nature and extent of epithelial functional recovery following injury is unknown.

As noted, vocal fold mucosal epithelial cells provide a physical and biochemical barrier to insults from the laryngeal lumen; this barrier function is largely modulated by cell adhesion molecules. For example, epithelial cadherin (E-cad), the major protein constituent of the epithelial cell junction, is responsible for restricting bacterial invasion [Villar et al., 2007] and directing the movement of water and other soluble molecules across the epithelium [reviewed by Gumbiner, 2005]. Transglutaminase (TGase)-1, a protein cross-linking enzyme, is an additional player in the regulation of epithelial permeability [Nemes et al., 1999]; however, TGase-1 overexpression can drive epithelial differentiation leading to squamous metaplasia [Martinet et al., 2003]. Epithelial cells also synthesize type IV collagen (Col-IV), a key structural constituent of the basement membrane that anchors epithelial cells to the underlying LP, promotes biomechanical stability, and provides an additional subepithelial barrier against unwanted mucosal invasion [Khoshnoodi et al., 2008]. These 3 molecules represent distinct features of functionally intact epithelium in a variety of tissues; therefore, an alteration in their abundance and distribution postinjury offers direct insight into the functional reestablishment (or lack thereof) of the epithelial barrier.

The majority of epithelial barrier function research has been conducted in nonlaryngeal tissues; consequently, a significant amount of knowledge concerning the vocal fold epithelium is inferred. The primary goal of this study, therefore, was to characterize the reestablishment of epithelial and basement membrane barrier structures following acute vocal fold mucosal injury, with a particular emphasis on E-cad, TGase-1, and Col-IV. We observed vocal fold epithelial barrier restoration characterized by active cell recruitment culminating in peak hyperplasia at 3 days postinjury, the establishment of robust E-cad and TGase-1 biochemical barrier signals along the epithelial surface by 3 days postinjury, and the absence of a Col-IV+ basement membrane at 7 days postinjury. The distinct spatial and temporal immunoactivity of these molecules is consistent with a programmed repair process driving the restoration of vocal fold mucosal integrity and permeability.

Materials and Methods

Animals

Twenty-one 4-month-old male Sprague-Dawley rats with a mean body weight of 290 g (±10 g) were used in this study. Sixteen rats received a unilateral vocal fold stripping injury, and 5 experimentally naïve rats were reserved as age-matched uninjured controls. All rats were housed in a pathogen-free facility at the University of Wisconsin School of Medicine and Public Health. All protocols involved in these experiments were approved by the Institutional Animal Care and Use Committee of the University of Wisconsin-Madison.

Surgery and Tissue Preparation

Vocal fold injuries were created as previously reported [Tateya et al., 2005; Ling et al., 2010]. In brief, rats underwent anesthesia induction using isoflurane inhalation (2–3% delivered at 0.8–1.5 l/min), followed by maintenance with an intraperitoneal injection of ketamine hydrochloride (90 mg/kg) and xylazine hydrochloride (9 mg/kg). Atropine sulfate (0.05 mg/kg) was also injected intraperitoneally to reduce the secretion of saliva and sputum in the laryngeal lumen. Under deep anesthesia, the rats were placed on an operation platform in a near vertical position, and a steel wire laryngoscope with a diameter of 1 mm was inserted to facilitate vocal fold exposure. A 25° rigid endoscope with a diameter of 1.9 mm (Richard Wolf, Vernon Hills, Ill., USA) connected to an external light source, and a video monitor was used for surgical monitoring. The right vocal fold mucosa was stripped using a 25-gauge needle, and injury was confirmed immediately by exposure of the thyroarytenoid muscle. Mucosal damage was consistent across experimental animals, and all rats recovered from surgery.

Euthanasia and laryngeal harvest were performed at 4 postinjury time points (4 rats per time point), i.e. 1, 3, 5, and 7 days postinjury. All animals (experimental and control) were euthanized via CO_2 asphyxiation, and their larynges were harvested.

The laryngeal specimens were immediately embedded in optimum cutting temperature compound (Tissue-Tek; Sakura, Tokyo, Japan), frozen with acetone and dry ice, and stored at –80°C. The larynges were sectioned at an interval of 8 μm in the coronal plane using a cryostat (CM-3050 S; Leica, Wetzlar, Germany). One hundred serial sections, encompassing the majority of the vocal fold mucosa, were prepared from each laryngeal specimen. Every tenth section was subjected to routine hematoxylin and eosin (HE) staining to evaluate cell and tissue morphology and to identify the anatomical context along the anterior-posterior (A-P) axis.

Light Microscopy and Stereological Analysis

We performed stereological analysis of the HE-stained vocal fold mucosal sections in both naïve control and postinjury conditions using Stereo Investigator (MicroBrightField, Inc., Williston, Vt., USA). Our analysis setup consisted of a Zeiss Axioplan 2 microscope (Carl Zeiss, Thornwood, N.Y., USA) equipped with a digital microscopy camera (Carl Zeiss), a motorized stage (XYZ controller; Ludl, Hawthorne, N.Y., USA), and a computer running Stereo Investigator software (MicroBrightField) for instrument control, image capture, and image analysis.

Two adjacent coronal sections containing the midmembranous vocal fold mucosa immediately anterior to the laryngeal alar cartilage were selected from each animal for stereological analysis. The midmembranous mucosa was selected as it is an important tissue region for vocal fold oscillation and was in the center of the tissue injury site in all injured samples; the laryngeal alar cartilage was selected as an anatomical landmark to ensure that all analyses were performed at a consistent A-P level in the coronal plane. For each HE-stained section, a contour was drawn around the border of the epithelium. An open circle was selected as a marker for each individual cell within the epithelium, and markers were attached to the contour to provide relative coordinates. 2-dimensional epithelial cross-sectional area and cell density were calculated, and a geomorphic map comprised of the contour and cell makers was exported for illustration and comparison within and across injury and control conditions.

Immunohistochemistry

Frozen sections were fixed in 4% paraformaldehyde, washed with phosphate-buffered saline, and incubated with Block-Ace (AbD Serotech, Raleigh, N.C., USA) and 5% goat serum (Sigma, St. Louis, Mo., USA) for 30 min to block nonspecific binding. Next, sections were sequentially incubated with primary antibodies [mouse monoclonal anti-E-cad, clone H-108, 2 μg/ml (Santa Cruz Biotechnology, Inc., Santa Cruz, Calif., USA); rabbit polyclonal anti-Col-IV, 10 μg/ml (Abcam, Cambridge, Mass., USA), and mouse monoclonal anti-TGase-1, clone B.C1, 1:100 dilution (Acris, Herford, Germany)] for 90 min, and rhodamine red conjugated goat anti-mouse or anti-rabbit IgG (1:200 dilution; Jackson ImmunoResearch, Inc., West Grove, Pa., USA) for 90 min, with thorough wash steps between each incubation. Finally, slides were covered with antifade mounting medium (Vector Labs, Burlingame, Calif., USA) with or without 4′,6-diamidino-2-phenylindole dihydrochloride (DAPI), and cover-slipped. Control sections stained with an isotype control or without the primary or secondary antibody showed no immunoreactivity (data not shown).

Fluorescent Microscopy

Immunostained images of each section were captured using a fluorescent microscope (E-600; Nikon, Melville, N.Y., USA) equipped with a digital microscopy camera (DP-71; Olympus, Center Valley, Pa., USA) at a magnification of 100× (for imaging the entire vocal fold mucosa) and 400× (for imaging detailed cell morphology). Consistent exposure parameters were used for each marker to allow the direct comparison of fluorescent intensity across experimental conditions. Representative images from each experimental condition were selected for presentation.

Statistical Analysis

Changes in the epithelial 2-dimensional cross-sectional area and cellular density postinjury were assessed using 1-way analysis of variance (ANOVA). Where indicated, post hoc comparisons were performed using Fisher's protected least significant difference method. Data were rank-transformed prior to analysis to better meet the assumptions of ANOVA. Analyses were performed using SAS 9.1.3 (SAS Institute, Cary, N.C., USA). An α-level of 0.05 was employed for all comparisons; all p values were 2-sided.

Results

Vocal Fold Epithelial Morphology and Cellular Composition

We first characterized epithelial morphology in naïve and injured rat vocal fold mucosa. On HE-stained sections, the epithelial layer was well distinguished from its underlying LP by a relatively dark appearance and distinctive cellular features (fig. 1). The superior and midpoint epithelial regions were comprised of 1 or 2 layers of stratified squamous cells (SSCs) (fig. 1b, c). This SSC formation gradually transitioned into a ciliated pseudocolumnar formation (CPF) (fig. 1d) towards the inferior boundary of the vocal fold and formed a seamless connection with the tracheal epithelium below. As a result, the number of cell layers and overall medial-lateral (M-L) thickness increased gradually along the epithelial S-I axis.

This well-defined epithelial structure was successfully removed by our mucosal stripping procedure (fig. 2b); complete reepithelialization occurred by 3 days postinjury in all animals (fig. 2c) [Ling et al., 2010]. Stereological analysis revealed a significant increase in the epithelial cross-sectional area from 3 to 5 days postinjury (fig. 2c–e), with peak expansion at 5 days postinjury ($p < 0.05$; fig. 2f). The total number of epithelial cells was comparable to the control at 3 days postinjury, and significantly increased at 5 and 7 days postinjury ($p < 0.05$; fig. 2g). Cell density in the newly reconstructed epithelium was significantly lower than in the control at all postinjury time points ($p < 0.05$) (fig. 2h) due to the cross-sectional area expansion exceeding the cell recruitment rate.

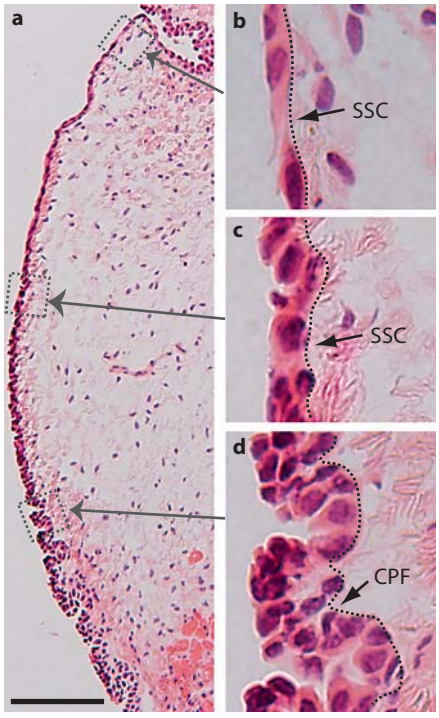

Fig. 1. Anatomical and morphological characteristics of the naïve rat vocal fold epithelium. **a** Microscopy image of an HE-stained coronal section illustrating the gross anatomy of the vocal fold mucosa. **b–d** Boxes in **a** have been enlarged for better illustration. The dotted contour line represents the boundary between the epithelium (left) and the LP (right). Scale bar = 200 μm (**a**) and 25 μm (**b–d**).

Immunolocalization of E-Cad

We employed immunohistochemistry to investigate the immunoactivity of E-cad, a calcium-dependent cell-cell adhesion molecule with an established role in epithelial barrier function [Gumbiner, 2005], in naïve and injured vocal fold mucosa. The E-cad immunoactivity in the naïve vocal fold was consistently restricted to the epithelial region and exhibited relatively low signal intensity in all animals examined (fig. 3a, 4a–c). Both cell surface (indicated by arrows in fig. 4a–c) and extracellular (indicated by arrowheads in fig. 4c) E-Cad signals were detected. E-cad+ cells were widely distributed throughout the most superficial epithelial cell layer along its S-I axis. Extracellular E-cad signals were predominantly located in the basement membrane.

One day postinjury, the majority of newly recruited epithelial cells were E-cad– (fig. 3b, indicated by arrows in fig. 4d–f); a small number of E-cad+ cells were observed in isolated clusters (indicated by a wide arrow in fig. 4d) near the superior and inferior poles. Diffuse low-intensity extracellular E-cad signals were noted among the mucosal debris present in the tissue (indicated by asterisks in fig. 3b). Additional extracellular E-cad signals exhibited an organized subepithelial distribution pattern in the region of expected basement membrane reconstruction (indicated by arrowheads in fig. 4e). Three days postinjury, reepithelialization was complete (fig. 2c) and strong E-cad signals were visualized on cells throughout the epithelial surface layer (fig. 3c, indicated by arrows in fig. 4g–i). Occasional diffuse signals were still detected among the residual mucosal debris (indicated by an asterisk in fig. 3c); some extracellular signal clusters were also observed in the deep epithelium (indicated by an arrow in fig. 3c). The increased number of E-cad+ cells on the epithelial surface layer was also present at 5 (fig. 3d, 4j–l) and 7 (fig. 3e, 4m–o) days postinjury, whereas extracellular E-cad signals were largely absent at these time points (fig. 3d, e).

Immunolocalization of TGase-1

To further examine the alteration in epithelial barrier function following vocal fold mucosal injury, we examined the immunoactivity of TGase-1, an enzyme triggered by a rise in intracellular calcium to catalyze the protein cross-linking necessary for epithelial mechanical integrity and water impermeability [Nemes et al., 1999]. In the naïve mucosa, TGase-1 signals were detected exclusively in superior epithelial region SSCs (fig. 5a). Comparable TGase-1 localization was observed in uninjured vocal folds contralateral to the mucosal injury site in all experimental animals. These signals were densely connected and formed a continuous biochemical structure along the superior epithelial region (fig. 5b, d, f). Within this region, TGase-1 was preferentially localized to the inner (i.e., deep or basal) SSC layer, leaving some superficial (possibly desquamating) cells exposed (indicated by arrows in fig. 5b, d, f). TGase-1 signals disappeared at the S-I transition from SSC to CPF (fig. 5a, c, e, g).

One day postinjury, the majority of newly recruited epithelial cells were TGase-1– (indicated by arrowheads in fig. 6b, 7e); a small number of TGase-1+ cells were present near the superior pole of the mucosa (possibly residual SSCs not removed by the stripping procedure; indicated by an arrow in fig. 6b). Additional TGase-1+ cells with a relatively low signal intensity were identified near the inferior pole of the mucosa, within the CPF region (indicated by wide arrows in fig. 6b, 7f). TGase-1 signals increased significantly at 3 and 5 days postinjury

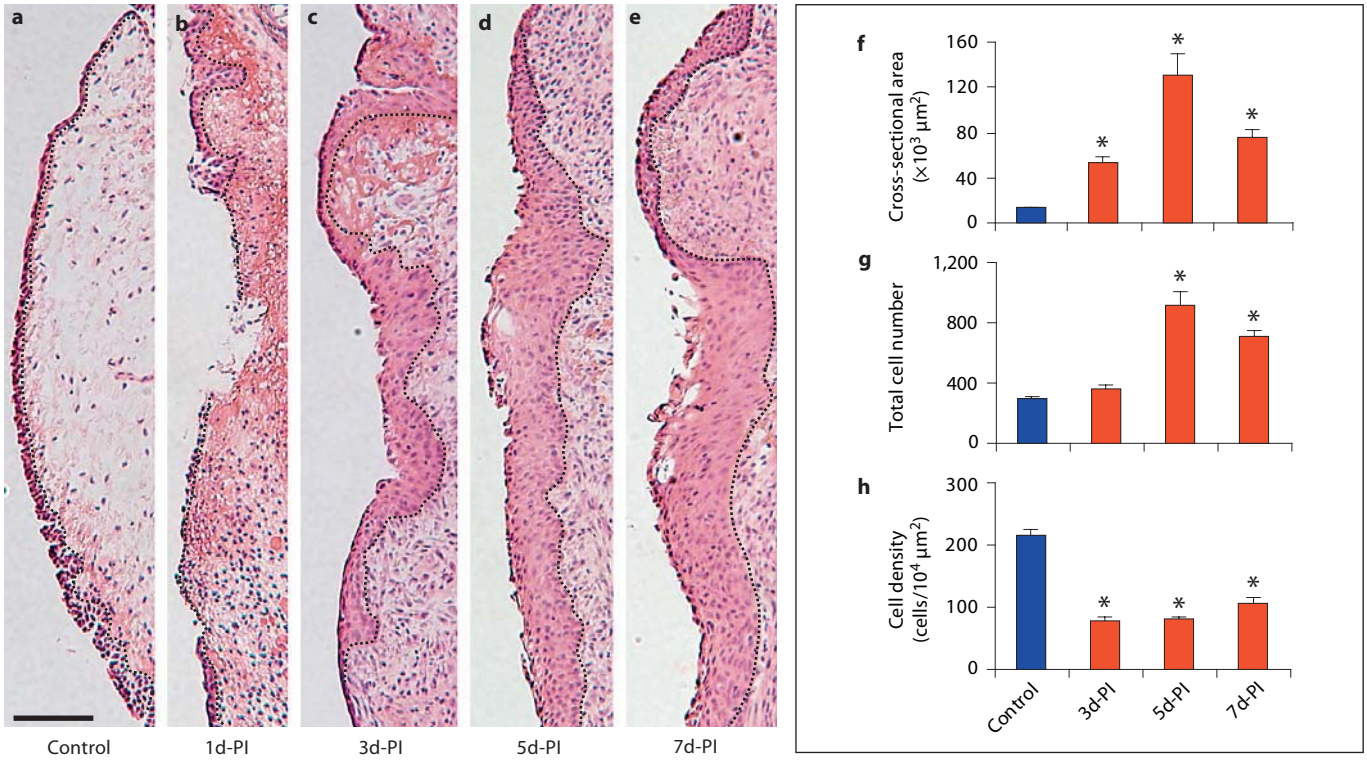

Fig. 2. Representative images of HE-stained coronal sections (**a–e**) and the corresponding stereological analysis (**f–h**) of changes in epithelial cross-sectional area and cell density following vocal fold mucosal injury. The dotted contour line in **a–e** represents the boundary between the epithelium (left) and the LP (right). Quantitative data in **f–h** are presented as means ± standard error. d-PI = Days postinjury. * $p < 0.05$ compared to the control. Scale bar = 200 μm.

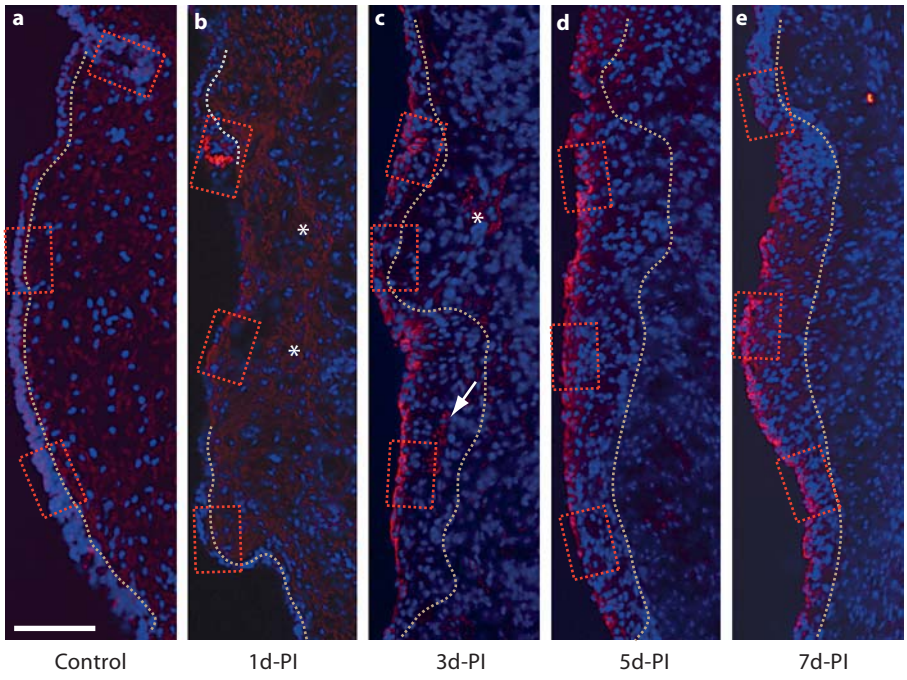

Fig. 3. Representative images illustrating changes in E-cad immunoactivity in the rat vocal fold mucosa following injury. Frozen coronal sections were stained with antibody anti-E-cad (red) and nuclear dye DAPI (blue). Merged images show E-cad signals primarily localized to the epithelium, with elevated signal intensity beginning at 3 days postinjury. The dotted contour line represents the boundary between the epithelium (left) and the LP (right). The boxes in each image have been enlarged for better illustration and are displayed in figure 4. **b**, **c** Asterisks indicate low-intensity extracellular E-cad signal clusters in the residual mucosal debris at 1–3 days postinjury; the arrow indicates an extracellular E-cad signal cluster in the deep epithelium at 3 days postinjury. d-PI = Days postinjury. Scale bar = 200 μm.

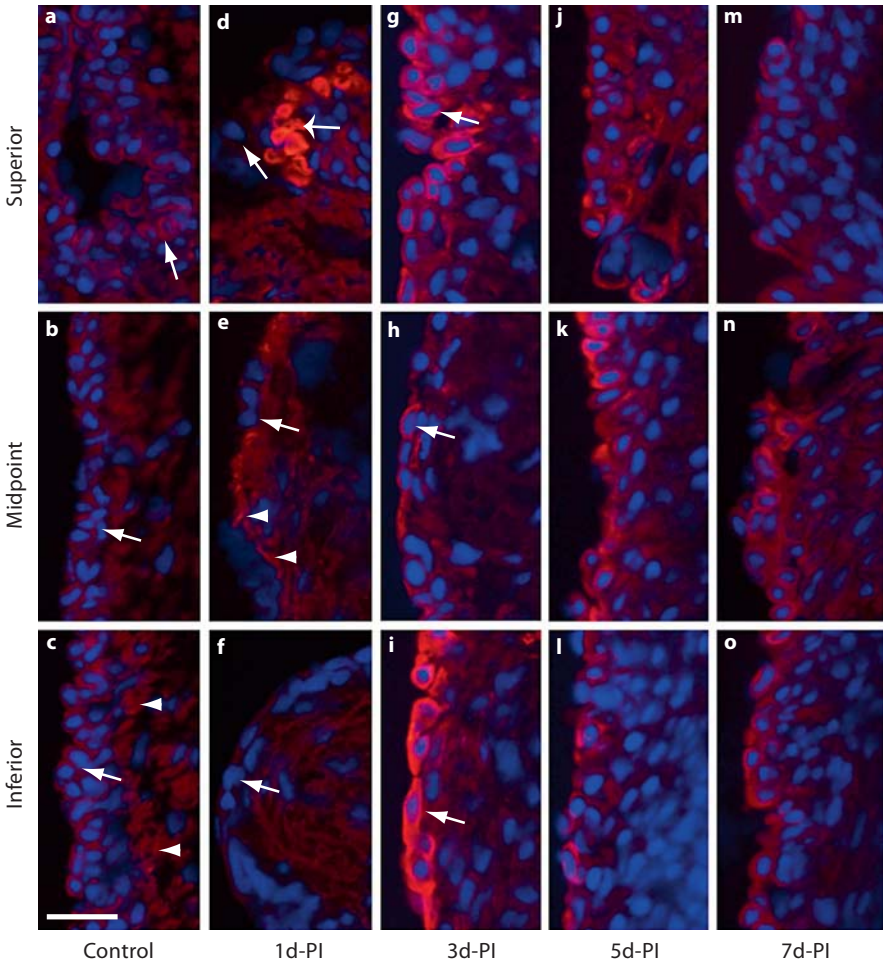

Fig. 4. High-magnification representative images (corresponding to the small red boxes in fig. 3) illustrating changes in E-cad immunoactivity in the rat vocal fold epithelium following injury. **a–c** Arrows indicate low-intensity E-cad+ cells in the naïve epithelium. **c** Arrowheads indicate low-intensity E-cad signals in the naïve basement membrane region. **d–f** Arrows indicate E-cad– epithelial cells 1 day postinjury. **d** The wide arrow indicates an isolated E-cad+ epithelial cell cluster at 1 day postinjury. **e** Arrowheads indicate subepithelial E-cad signals at 1 day postinjury. **g–i** Arrows indicate E-cad+ epithelial cells at 3 days postinjury. d-PI = Days postinjury. Scale bar = 20 μm.

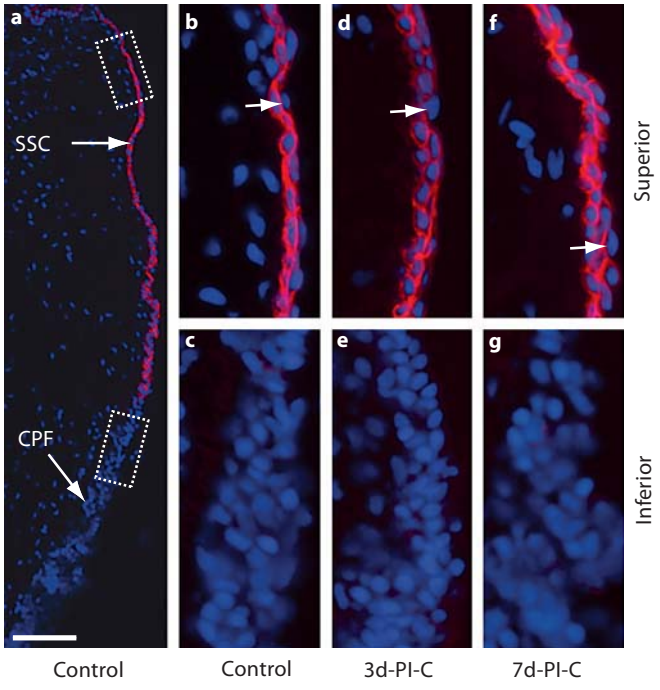

Fig. 5. Representative images illustrating TGase-1 immunoactivity in the naïve rat vocal fold epithelium and uninjured epithelium contralateral to the mucosal injury site. Frozen coronal sections were stained with antibody anti-TGase-1 (red) and nuclear dye DAPI (blue). Merged images show TGase-1 signals exclusively localized to the SSC epithelial region and absent in the CPF epithelial region. Boxes in **a** have been enlarged for better illustration and are displayed in **b** and **c**. **d–g** Comparable anatomical locations. **b**, **d**, **f** Arrows indicate epithelial cells in TGase-1+ nests exposed to the lumen. PI-C = Postinjury contralateral (uninjured) control. Scale bar = 200 μm (**a**) and 20 μm (**b–g**).

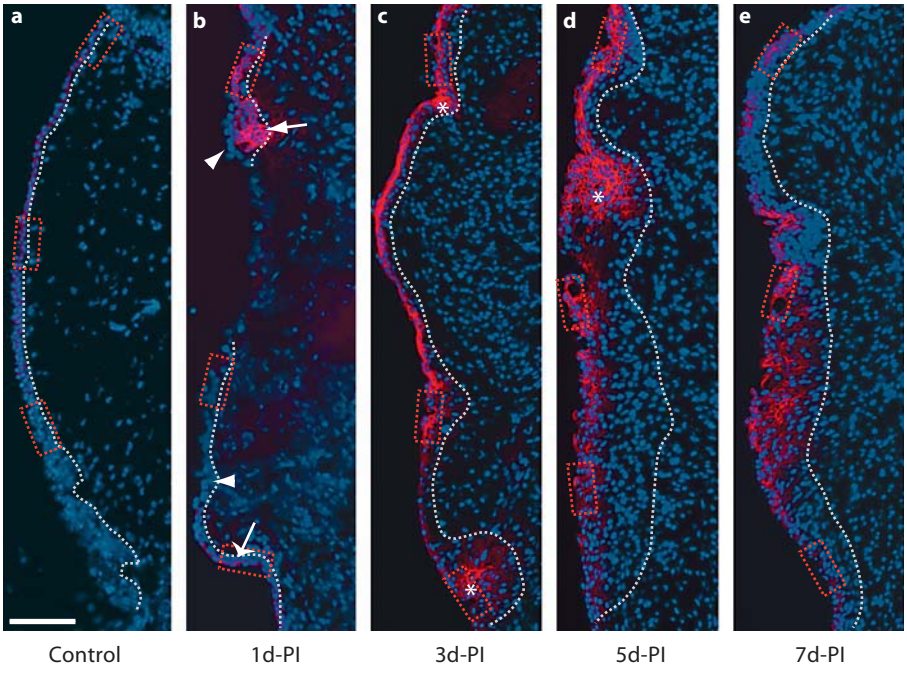

Fig. 6. Representative images illustrating changes in TGase-1 immunoactivity in the rat vocal fold epithelium following mucosal injury. Frozen coronal sections were stained with antibody anti-TGase-1 (red) and nuclear dye DAPI (blue). Merged images show a significant change in TGase-1 expression postinjury. The dotted contour line represents the boundary between the epithelium (left) and the LP (right). The boxes in each image have been enlarged for better illustration and are displayed in figure 7. **b** The arrow indicates a cluster of superior-region TGase-1+ epithelial cells at 1 day postinjury. The wide arrow indicates inferior-region TGase-1+ epithelial cells at 1 day postinjury, and arrowheads indicate TGase-1– epithelial cells at 1 day postinjury. **c**, **d** Asterisks indicate TGase-1+ epithelial cell clusters at 3–5 days postinjury. d-PI = Days postinjury. Scale bar = 200 μm.

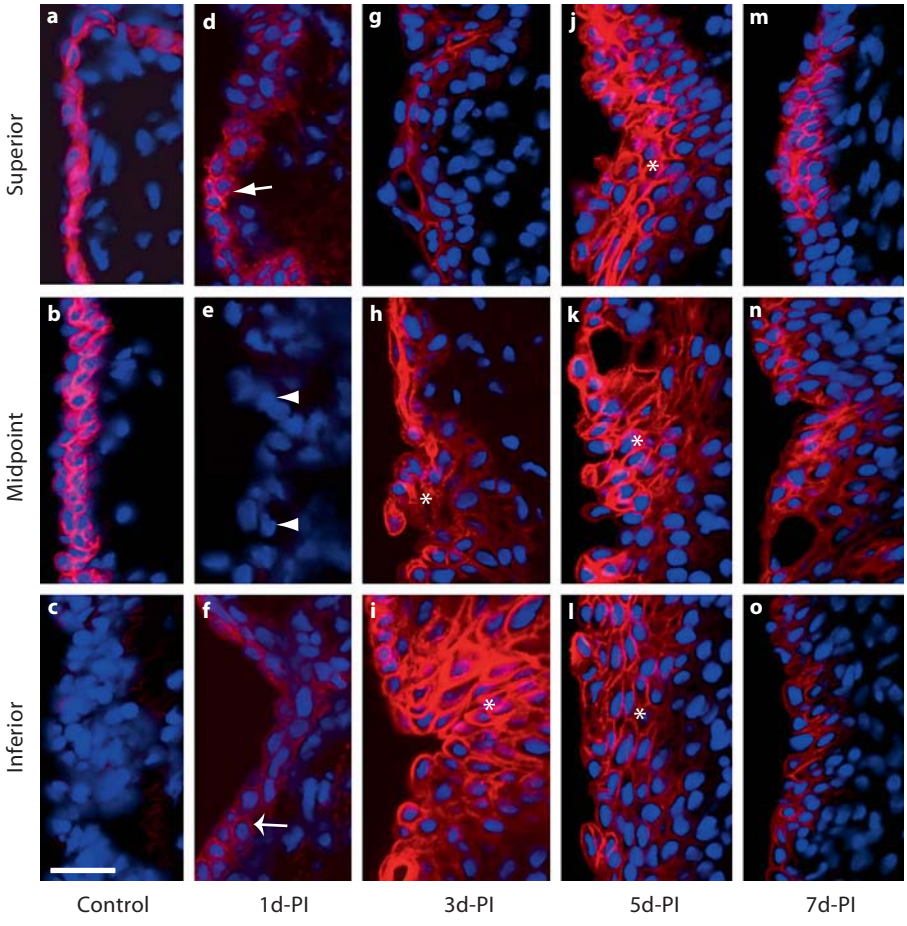

Fig. 7. High-magnification representative images (corresponding to the small red boxes in fig. 6) illustrating changes in TGase-1 immunoactivity in the rat vocal fold epithelium following injury. **d** Arrow indicates superior-region TGase-1+ epithelial cells at 1 day postinjury. **e** Arrowheads indicate midpoint-region TGase-1– epithelial cells at 1 day postinjury. **f** The wide arrow indicates inferior-region TGase-1+ epithelial cells at 1 day postinjury. **h–l** Asterisks indicate TGase-1+ epithelial cell clusters at 3–5 days postinjury. d-PI = Days postinjury. Scale bar = 20 μm.

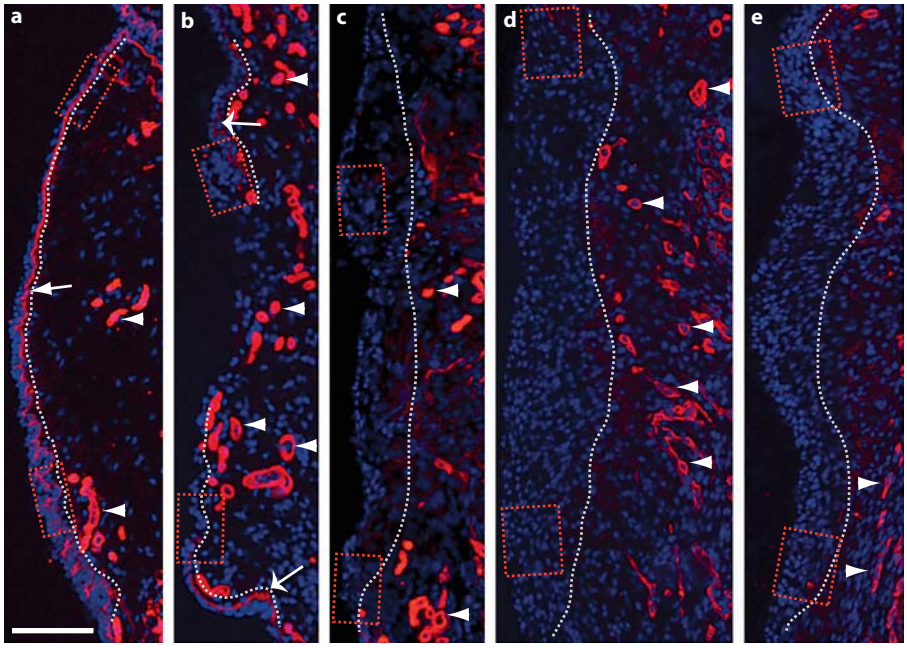

Fig. 8. Representative images illustrating changes in Col-IV immunoactivity in the rat vocal fold mucosa following injury. Frozen coronal sections were stained with antibody anti-Col-IV (red) and nuclear dye DAPI (blue). Merged images show a significant change in Col-IV expression postinjury. The dotted contour line represents the boundary between the epithelium (left) and LP (right). The boxes in each image have been enlarged for better illustration and are displayed in figure 9. **a** The arrow indicates a Col-IV+ subepithelial basement membrane structure in the naïve mucosa. **a–e** Arrowheads indicate Col-IV+ vascular basement membrane structures in naïve and injured mucosa. **b** Wide arrows indicate residual Col-IV+ subepithelial basement membrane fragments 1 day postinjury. d-PI = Days postinjury. Scale bar = 200 μm.

and were detected across the entire epithelium (fig. 6c, d, 7g–l). Signal intensity and distribution varied considerably by region; some large TGase-1+ cell clusters were observed (indicated by asterisks in fig. 6c, d, 7h–l). TGase-1 exhibited a similar distribution pattern with a slightly reduced signal intensity at 7 days postinjury (fig. 6e, 7m–o).

Immunolocalization of Col-IV

We examined Col-IV immunoactivity to evaluate the reconstruction of the basement membrane and the reestablishment of epithelial cell anchoring following vocal fold mucosal injury. A Col-IV+ basement membrane structure 1–3 μm in thickness was identified in the naïve mucosa (indicated by arrows in fig. 8a, 9a, b). Additional Col-IV signals were observed in the LP and exhibited vessel-like morphology (indicated by arrowheads in fig. 8a). Our mucosal stripping procedure removed the majority of the basement membrane; however, residual Col-IV+ structures were observed near the superior and inferior mucosal poles at 1 day postinjury (indicated by wide arrows in fig. 8b, 9c, d). These residual structures were absent at all subsequent time points (fig. 8c–e), suggesting an active degenerative process. An increased number of Col-IV+ vessel-like structures were identified in the LP at all postinjury time points compared to the naïve control (indicated by arrowheads in fig. 8b–e), consistent with injury-induced angiogenesis. Emerging Col-IV+ structures were identified in the deep region of the newly reconstructed epithelium between 3 and 7 days postinjury (indicated by arrowheads in fig. 9e–j).

Discussion

The primary goal of this study was to evaluate the reestablishment of epithelial and basement membrane barrier structures following vocal fold mucosal injury. The vocal fold epithelium is critical to upper airway immunologic defense [Thibeault et al., 2009] and water/ion transport [Fisher et al., 2001]; therefore, any form of physical trauma or insult increases the vulnerability of this structure to functional impairment and pathogen invasion/infection. We observed complete mucosal reepithelialization by 3 days postinjury, as previously reported [Ling et al., 2010]. Epithelial reconstruction was characterized by active cell recruitment and tissue expansion culminating in hyperplasia between 3 and 7 days postinjury. Differential immunoactivity of E-cad, TGase-1, and Col-IV was observed in the naïve and injured epithelium-basement membrane complex, suggesting region-specific functional roles for these molecules in the regulation of vocal fold mucosal integrity and permeability. We observed the return of E-cad+ and TGase-1+ bio-

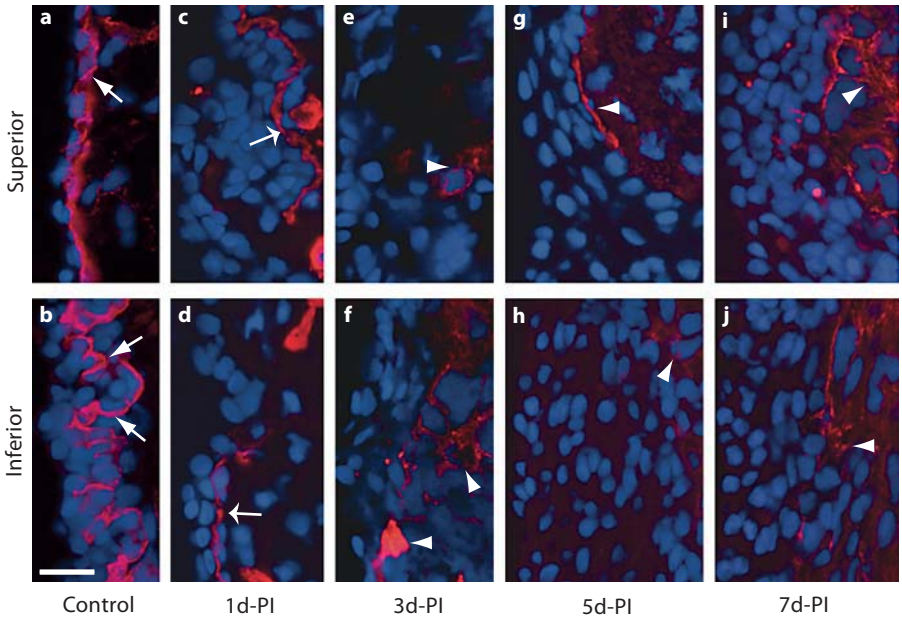

Fig. 9. High-magnification representative images (corresponding to the small red boxes in fig. 8) illustrating changes in Col-IV immunoactivity in the rat vocal fold mucosa following injury. **a**, **b** Arrows indicate a Col-IV+ subepithelial basement membrane structure in the naïve mucosa. **c**, **d** Wide arrows indicate residual Col-IV+ subepithelial basement membrane fragments 1 day postinjury. **e–j** Arrowheads indicate emerging Col-IV+ structures in the deep epithelium at 3–7 days postinjury. d-PI = Days postinjury. Scale bar = 20 μm.

chemical barriers within 7 days postinjury; however, Col-IV+ basement membrane regeneration did not occur during this time period.

Vocal fold mucosal repair studies have traditionally focused on the LP and its extracellular matrix [Kurita, 1983; Hirano et al., 1999; Gray, 2000; Rousseau et al., 2003; Hansen and Thibeault, 2006; Lim et al., 2006; Tateya et al., 2006a; Welham et al., 2008]; in contrast, relatively little attention has been given to the cellular and biochemical features of vocal fold epithelial reconstruction [Tateya et al., 2006b; Ling et al., 2010]. The cell recruitment and epithelial expansion observed here appear to reflect a sequential and programmed repair process. Early hyperplasia may provide some level of protection against pathogens and other irritating agents, but may also impact epithelial transport efficiency and contribute to an increased vocal fold mass. While active cell recruitment and proliferation are desirable tissue repair processes, excessive or abnormal hyperplasia is undesirable. Previous work in rat vocal fold mucosal injury suggests that injury-induced epithelial hyperplasia is attenuated by 14 days postinjury [Tateya et al., 2006b].

E-cad is the most widely studied protein in the calcium-dependent adhesion molecule (cadherin) superfamily. It contributes to adherent junction assembly and formation of the epithelial junctional complex [Gumbiner, 2005]. This junctional complex serves as a site of cell-cell and cell-basement membrane adhesion and acts as a barrier to prevent the flow of water, soluble molecules, and bacteria through the intercellular space [Gumbiner, 2005; Villar et al., 2007]. E-cad interacts with many other proteins in the junctional complex, including the claudins and occludins, and is able to increase the strength and stability of the complex via catenin-modulated binding to the actin cytoskeleton [van Roy et al., 2008]. E-cad is critical to the maintenance of mucosal integrity and has been shown to play a defensive role in response to nasal [Arican et al., 2009] and laryngeal [Gill et al., 2005; Sivasankar et al., 2010] mucosal challenges. In this study, we identified strong E-cad immunoactivity in cells along the luminal surface of the newly reconstructed epithelium postinjury. E-cad expression was largely localized to the most superficial epithelial cell layer. These results suggest that E-cad is important to vocal fold mucosal integrity and that reestablishment of the epithelial junctional complex is an early tissue repair target. The new epithelium may regain, at least in part, its function as an immunologic and physiologic barrier as early as 3 days postinjury.

TGase-1 catalyzes epithelial protein cross-linking, which in turn confers tissue stability and resistance to chemical, enzymatic, and biomechanical disruption [Greenberg et al., 1991]. This enzyme also influences keratinocyte differentiation and is essential to the water impermeability of skin [Candi et al., 2005; Segre, 2006]. In addition to being expressed in the epidermis, TGase-1 is expressed in nonkeratinized epithelium [Floyd and Jetten, 1989; Lotan, 1993; Martinet et al., 2003] such as

that which is seen in the vocal fold. We observed exclusive TGase-1 localization to the SSC region of the naïve vocal fold epithelium, suggesting that this enzyme plays a regulatory role in squamous differentiation. Previous work has shown moderate TGase-1 expression in naïve rat vocal fold epithelium as well as significant upregulation (with metaplasia) in response to vitamin A deficiency [Tateya et al., 2008], inferring that vitamin A acts to inhibit TGase-1 synthesis and metaplastic progression within this tissue. Related work in corneal [Nishida et al., 1999], bronchial [Martinet et al., 2003; Dakir et al., 2008], hepatic [Hiiragi et al., 1999], and renal [Hiiragi et al., 1999] epithelia has also identified a link between TGase-1 upregulation and aberrant squamous differentiation leading to metaplasia; again, this process appears to be inhibited by vitamin A and its retinoid analogs [Jetten et al., 1987; Lotan, 1993].

E-cad and TGase-1 colocalization has been reported in liver, kidney, and simple epithelial cell monolayer cultures; in each case TGase-1 cross-linking activity appears to be concentrated around E-cad-based epithelial junctional complexes [Hiiragi et al., 1999]. Consistent with these findings, we observed both TGase-1 and E-cad signals in the intercellular space between SSCs in the naïve vocal fold epithelium. Within this SSC region, low-intensity E-cad signals were widely distributed throughout the entire epithelial cell layer and its adjacent basement membrane; high-intensity TGase-1 signals surrounded all but a few luminal surface epithelial cells and did not extend to the basement membrane. E-cad was expressed in both SSC and CPF epithelial regions, whereas TGase-1 was exclusively expressed in the SSC region. Following injury, we observed rapid E-cad synthesis and localization to the luminal epithelial surface, alongside preferential TGase-1 localization to large patches throughout the depth of the epithelium. These distinct epithelial distribution patterns in both naïve and injured mucosa support the functional specificity of these 2 molecules in the vocal fold. E-cad appears to provide an immediate defensive barrier at the interface between the epithelium and laryngeal lumen (but still deep to the protective layer of surface liquid/mucus [Gray, 2000; Leydon et al., 2009]), whereas TGase-1, the most important barrier regulator in epidermis [Candi et al., 2005; Segre, 2006], may play a complementary defensive role at a slightly deeper anatomic level.

TGase-1 activation is critical to dermal wound healing [Inada et al., 2000], pathologic squamous differentiation of tracheal and bronchial epithelia [Floyd and Jetten, 1989; Martinet et al., 2003], and the maintenance of simple epithelial cells in culture [Martinet et al., 2003]. It also regulates the survival and proliferation of renal epithelial cells, essential processes for renal regeneration [Ponnusamy et al., 2009; Zhang et al., 2009]. Consistent with these reports, we observed strong TGase-1 expression in both residual and newly recruited vocal fold epithelial cells postinjury. It is of particular interest that TGase-1 signals were observed in the normally TGase-1– CPF epithelial region, suggesting that the mucosal injury response overcomes any CPF-associated TGase-1 inhibition. A number of lymphocytes and inflammatory cytokines present following vocal fold mucosal injury [Lim et al., 2006; Welham et al., 2008]; some, such as interferon-γ, are known inducers of TGase-1 [Saunders and Jetten, 1994] and may have contributed to the effect observed here.

Col-IV is a key protein constituent of the basement membrane. In mucosal tissues such as the vocal fold, the basement membrane anchors the epithelium to its underlying LP and provides a subepithelial barrier against unwanted mucosal invasion [Hirano and Kakita, 1985; Gray, 2000]. In blood vessels, the Col-IV-rich basement membrane is synthesized during angiogenesis and surrounds endothelial cells and pericytes [Baluk et al., 2003; Hamano et al., 2003]. In this study, we observed both subepithelial and subendothelial Col-IV signals in naïve and injured vocal fold mucosa. The Col-IV+ basement membrane identified in the naïve mucosa was removed by our injury procedure and failed to regenerate by 7 days postinjury despite complete reepithelialization by 3 days postinjury. In contrast, we observed a significant increase in Col-IV signals around vascular walls in the LP postinjury, indicative of active angiogenesis. These results suggest that Col-IV synthesis is more rapidly induced in endothelial cells compared to epithelial cells following vocal fold mucosal injury, and that mucosal basement membrane reconstruction is a relatively late-occurring tissue repair event.

We previously reported the return of squamous cell stratification in the reconstructed vocal fold epithelium by 7 days postinjury and suggested that this morphological transformation might correspond to epithelial functional recovery [Ling et al., 2010]. Our current data provide greater insight into the reestablishment of epithelial barrier function, demonstrating active cell recruitment leading to peak hyperplasia 3 days postinjury, robust E-cad and TGase-1 biochemical signals along the epithelial surface by 3 days postinjury, and the absence of a Col-IV+ basement membrane at 7 days postinjury. The distinct spatial and temporal immunoactivity of these molecules is consistent with a programmed repair process driving the restoration of vocal fold mucosal integrity and per-

meability; however, additional work is needed to establish the natural course of basement membrane regeneration. These data may inform future efforts to optimize functional mucosal recovery postinjury and to avoid undesirable events such as pathogen invasion/infection or epithelial metaplasia.

Acknowledgements

This work was supported by grant R01 DC004428 from the National Institute on Deafness and Other Communicative Disorders (NIDCD). We gratefully acknowledge the statistical consultation provided by Glen Leverson, PhD.

References

Arican, R.Y., Z. Sahin, I. Ustunel, L. Sarikcioglu, S. Ozdem, N. Oguz (2009) Effects of formaldehyde inhalation on the junctional proteins of nasal respiratory mucosa of rats. Exp Toxicol Pathol *61:* 297–305.

Baluk, P., S. Morikawa, A. Haskell, M. Mancuso, D.M. McDonald (2003) Abnormalities of basement membrane on blood vessels and endothelial sprouts in tumors. Am J Pathol *163:* 1801–1815.

Birchall, M.A., M. Bailey, D. Gutowska-Owsiak, N. Johnston, C.F. Inman, C.R. Stokes, G. Postma, L. Pazmany, J.A. Koufman, A. Phillips, L.E. Rees (2008) Immunologic response of the laryngeal mucosa to extraesophageal reflux. Ann Otol Rhinol Laryngol *117:* 891–895.

Bulmer, D.M., M.S. Ali, I.A. Brownlee, P.W. Dettmar, J.P. Pearson (2010) Laryngeal mucosa: its susceptibility to damage by acid and pepsin. Laryngoscope *120:* 777–782.

Candi, E., R. Schmidt, G. Melino (2005) The cornified envelope: a model of cell death in the skin. Nat Rev Mol Cell Biol *6:* 328–340.

Dakir, E.L., L. Feigenbaum, R.I. Linnoila (2008) Constitutive expression of human keratin 14 gene in mouse lung induces premalignant lesions and squamous differentiation. Carcinogenesis *29:* 2377–2384.

Dworkin, J.P., P.M. Reidy, R.J. Stachler, J.H. Krouse (2009) Effects of sequential *Dermatophagoides pteronyssinus* antigen stimulation on anatomy and physiology of the larynx. Ear Nose Throat J *88:* 793–799.

Fisher, K.V., A. Telser, J.E. Phillips, D.B. Yeates (2001) Regulation of vocal fold transepithelial water fluxes. J Appl Physiol *91:* 1401–1411.

Floyd, E.E., A.M. Jetten (1989) Regulation of type I (epidermal) transglutaminase mRNA levels during squamous differentiation: down regulation by retinoids. Mol Cell Biol *9:* 4846–4851.

Gill, G.A., N. Johnston, A. Buda, M. Pignatelli, J. Pearson, P.W. Dettmar, J. Koufman (2005) Laryngeal epithelial defenses against laryngopharyngeal reflux: investigations of E-cadherin, carbonic anhydrase isoenzyme III, and pepsin. Ann Otol Rhinol Laryngol *114:* 913–921.

Gray, S.D. (2000) Cellular physiology of the vocal folds. Otolaryngol Clin North Am *33:* 679–697.

Gray, S.D., I.R. Titze, F. Alipour, T.H. Hammond (2000) Biomechanical and histologic observations of vocal fold fibrous proteins. Ann Otol Rhinol Laryngol *109:* 77–85.

Gray, S.D., I.R. Titze, R. Chan, T.H. Hammond (1999) Vocal fold proteoglycans and their influence on biomechanics. Laryngoscope *109:* 845–854.

Greenberg, C.S., P.J. Birckbichler, R.H. Rice (1991) Transglutaminases: multifunctional cross-linking enzymes that stabilize tissues. FASEB J *5:* 3071–3077.

Gumbiner, B.M. (2005) Regulation of cadherin-mediated adhesion in morphogenesis. Nat Rev Mol Cell Biol *6:* 622–634.

Hamano, Y., M. Zeisberg, H. Sugimoto, J.C. Lively, Y. Maeshima, C. Yang, R.O. Hynes, Z. Werb, A. Sudhakar, R. Kalluri (2003) Physiological levels of tumstatin, a fragment of collagen IV alpha 3 chain, are generated by MMP-9 proteolysis and suppress angiogenesis via alphaV beta3 integrin. Cancer Cell *3:* 589–601.

Hansen, J.K., S.L. Thibeault (2006) Current understanding and review of the literature: vocal fold scarring. J Voice *20:* 110–120.

Hiiragi, T., H. Sasaki, A. Nagafuchi, H. Sabe, S.C. Shen, M. Matsuki, K. Yamanishi, S. Tsukita (1999) Transglutaminase type 1 and its cross-linking activity are concentrated at adherence junctions in simple epithelial cells. J Biol Chem *274:* 34148–34154.

Hirano, M., Y. Kakita (1985) Cover-body theory of vocal fold vibration; in Daniloff, R.G. (ed): Speech Science: Recent Advances. San Diego, College-Hill, pp 1–46.

Hirano, M., K. Sato, T. Nakashima (1999) Fibroblasts in human vocal fold mucosa. Acta Otolaryngol *119:* 271–276.

Inada, R., M. Matsuki, K. Yamada, Y. Morishima, S.C. Shen, N. Kuramoto, H. Yasuno, K. Takahashi, Y. Miyachi, K. Yamanishi (2000) Facilitated wound healing by activation of the Transglutaminase 1 gene. Am J Pathol *157:* 1875–1882.

Jetten, A.M., A.R. Brody, M.A. Deas, G.E. Hook, J.I. Rearick, S.M. Thacher (1987) Retinoic acid and substratum regulate the differentiation of rabbit tracheal epithelial cells into squamous and secretory phenotype: morphological and biochemical characterization. Lab Invest *56:* 654–664.

Johnston, N., C.W. Wells, J.H. Blumin, R.J. Toohill, A.L. Merati (2007) Receptor-mediated uptake of pepsin by laryngeal epithelial cells. Ann Otol Rhinol Laryngol *116:* 934–938.

Khoshnoodi, J., V. Pedchenko, B.G. Hudson (2008) Mammalian collagen IV. Microsc Res Tech *71:* 357–370.

Khosla, S., S. Murugappan, E. Gutmark (2008) What can vortices tell us about vocal fold vibration and voice production. Curr Opin Otolaryngol Head Neck Surg *16:* 183–187.

Khosla, S., S. Murugappan, R. Paniello, J. Ying, E. Gutmark (2009) Role of vortices in voice production: normal versus asymmetric tension. Laryngoscope *119:* 216–221.

Kurita, S., K. Nagata, M. Hirano (1983) A comparative study of the layer structure of the vocal fold; in Bless, D.M., J.H. Abbs (eds): Vocal Fold Physiology: Contemporary Research and Clinical Issues. San Diego, College-Hill, pp 3–21.

Leydon, C., M. Sivasankar, D.L. Falciglia, C. Atkins, K.V. Fisher (2009) Vocal fold surface hydration: a review. J Voice *23:* 658–665.

Lim, X., I. Tateya, T. Tateya, A. Muñoz-Del-Río, D.M. Bless (2006) Immediate inflammatory response and scar formation in wounded vocal folds. Ann Otol Rhinol Laryngol *115:* 921–929.

Ling, C., M. Yamashita, E.A. Waselchuk, J.L. Raasch, D.M. Bless, N.V. Welham (2010) Alteration in cellular morphology, density and distribution in rat vocal fold mucosa following injury. Wound Repair Regen *18:* 89–97.

Lotan, R. (1993) Squamous cell differentiation markers in normal, premalignant, and malignant epithelium: effects of retinoids. J Cell Biochem Suppl *17F:* 167–174.

Martinet, N., L. Bonnard, V. Regnault, E. Picard, L. Burke, J. Siat, G. Grosdidier, Y. Martinet, J.M. Vignaud (2003) In vivo transglutaminase type 1 expression in normal lung, preinvasive bronchial lesions, and lung cancer. Am J Respir Cell Mol Biol *28:* 428–435.

Mouadeb, D.A., P.C. Belafsky, M. Birchall, C. Hood, T. Konia, K.E. Pinkerton (2009) The effects of allergens and tobacco smoke on the laryngeal mucosa of guinea pigs. Otolaryngol Head Neck Surg *140:* 493–497.

Nemes, Z., L.N. Marekov, L. Fesus, P.M. Steinert (1999) A novel function for transglutaminase 1: attachment of long-chain omega-hydroxyceramides to involucrin by ester bond formation. Proc Natl Acad Sci USA *96:* 8402–8407.

Nishida, K., K. Yamanishi, K. Yamada, A. Dota, S. Kawasaki, A.J. Quantock, S. Kinoshita (1999) Epithelial hyperproliferation and transglutaminase 1 gene expression in Stevens-Johnson syndrome conjunctiva. Am J Pathol *154:* 331–336.

Ponnusamy, M., M. Pang, P.K. Annamaraju, Z. Zhang, R. Gong, Y.E. Chin, S. Zhuang (2009) Transglutaminase-1 protects renal epithelial cells from hydrogen peroxide-induced apoptosis through activation of STAT3 and AKT signaling pathways. Am J Physiol Renal Physiol *297:* F1361–1370.

Rousseau, B., S. Hirano, T.D. Scheidt, N.V. Welham, S.L. Thibeault, R.W. Chan, D.M. Bless (2003) Characterization of vocal fold scarring in a canine model. Laryngoscope *113:* 620–627.

Saunders, N.A., A.M. Jetten (1994) Control of growth regulatory and differentiation-specific genes in human epidermal keratinocytes by interferon gamma: antagonism by retinoic acid and transforming growth factor beta 1. J Biol Chem *269:* 2016–2022.

Segre, J.A. (2006) Epidermal barrier formation and recovery in skin disorders. J Clin Invest *116:* 1150–1158.

Sivasankar, M., E. Erickson, M. Rosenblatt, R.C. Branski (2010) Hypertonic challenge to porcine vocal folds: effects on epithelial barrier function. Otolaryngol Head Neck Surg *142:* 79–84.

Sivasankar, M., K.V. Fisher (2007) Vocal fold epithelial response to luminal osmotic perturbation. J Speech Lang Hear Res *50:* 886–898.

Tateya, I., T. Tateya, X. Lim, J.H. Sohn, D.M. Bless (2006a) Cell production in injured vocal folds: a rat study. Ann Otol Rhinol Laryngol *115:* 135–143.

Tateya, I., T. Tateya, R.L. Surles, K. Kanehira, S. Tanumihardjo, D.M. Bless (2008) Vitamin A deficiency causes metaplasia in vocal fold epithelium: a rat study. Ann Otol Rhinol Laryngol *117:* 153–158.

Tateya, T., I. Tateya, J.H. Sohn, D.M. Bless (2005) Histologic characterization of rat vocal fold scarring. Ann Otol Rhinol Laryngol *114:* 183–191.

Tateya, T., I. Tateya, J.H. Sohn, D.M. Bless (2006b) Histological study of acute vocal fold injury in a rat model. Ann Otol Rhinol Laryngol *115:* 285–292.

Thibeault, S.L., L. Rees, L. Pazmany, M.A. Birchall (2009) At the crossroads: mucosal immunology of the larynx. Mucosal Immunol *2:* 122–128.

Villar, C.C., H. Kashleva, C.J. Nobile, A.P. Mitchell, A. Dongari-Bagtzoglou (2007) Mucosal tissue invasion by *Candida albicans* is associated with E-cadherin degradation, mediated by transcription factor Rim101p and protease Sap5p. Infect Immun *75:* 2126–2135.

van Roy, F., G. Berx (2008) The cell-cell adhesion molecule E-cadherin. Cell Mol Life Sci *65:* 3756–3788.

Welham, N.V., X. Lim, I. Tateya, D.M. Bless (2008) Inflammatory factor profiles one hour following vocal fold injury. Ann Otol Rhinol Laryngol *117:* 145–152.

Zhang, Z., J. Xing, L. Ma, R. Gong, Y.E. Chin, S. Zhuang (2009) Transglutaminase-1 regulates renal epithelial cell proliferation through activation of Stat-3. J Biol Chem *284:* 3345–3353.